Jul 1st, 12:00 AM

Air Pollutant Dispersion from a Large Semi-Enclosed Stadium in an Urban Area: High-Resolution CFD Modeling versus Full-Scale Measurements

Twan Van Hooff

Bert Blocken

International Environmental Modelling and Software Society (iEMSs)
2012 International Congress on Environmental Modelling and Software
Managing Resources of a Limited Planet, Sixth Biennial Meeting, Leipzig, Germany
R. Seppelt, A.A. Voinov, S. Lange, D. Bankamp (Eds.)
http://www.iemss.org/society/index.php/iemss-2012-proceedings

Air Pollutant Dispersion from a Large Semi-Enclosed Stadium in an Urban Area: High-Resolution CFD Modeling versus Full-Scale Measurements

Twan van Hooff[a,b], Bert Blocken[a]
[a]*Unit Building Physics and Services, Department of the Built Environment, Eindhoven University of Technology, Eindhoven, The Netherlands*
[b]*Division of Building Physics, Department of Civil Engineering, KU Leuven, Belgium*
b.j.e.blocken@tue.nl

Abstract: High-resolution CFD simulations and full-scale measurements have been performed to assess the dispersion of air pollutants (CO_2) from the large semi-enclosed Amsterdam ArenA football stadium. The dispersion process is driven by natural ventilation by the urban wind flow and by buoyancy, and by the interaction between outdoor wind flow and indoor airflow which are only connected by the relatively small ventilation openings in the stadium facade. The CFD simulations are performed with the 3D Reynolds-averaged Navier-Stokes equations supplemented with the realizable k-ε model to provide closure. The full-scale measurements include reference wind speed, wind direction, and outdoor and indoor air temperature, water vapor and indoor CO_2 concentration. In particular, the focus is on CFD simulations and measurements for the few hours immediately after a concert, when the stadium roof remains closed and when indoor air temperature, water vapor and CO_2 concentration have reached a maximum level due to the attendants. The removal of the sources/attendants allows an assessment of the natural ventilation rate using the concentration decay method. The CFD simulations compare favorably with the measurements in terms of mean wind velocity in the main ventilation openings and in terms of the CO_2 concentration decay after the concerts. The validated CFD model will in the future be used for a detailed evaluation of indoor concentration gradients and the interaction between wind-induced and buoyancy-induced natural ventilation.

Keywords: Computational Fluid Dynamics (CFD); natural ventilation; buoyancy; stadium aerodynamics.

1 INTRODUCTION

The removal of contaminants from buildings is important for indoor air quality and for the comfort and health of the occupants. Natural ventilation by wind and buoyancy is a sustainable approach for removal of contaminants [e.g. Linden 1999, Hunt and Linden 1999, Li and Delsante 2001]. One of the available methods to analyze natural ventilation of buildings is Computational Fluid Dynamics (CFD) [e.g. Heiselberg et al. 2004, Chen 2009, van Hooff and Blocken 2010, Ramponi and Blocken 2012]. However, the accuracy and reliability of CFD are important concerns. Therefore, CFD verification and validation are imperative [e.g. Casey and Wintergerste 2000, Jakeman et al. 2006, Franke et al. 2004, 2007, Tominaga et al. 2008, Chen 2009, Blocken et al. 2012, Blocken and Gualtieri 2012]. This requires high-quality experimental data, either wind tunnel data or field data. These data in turn need to satisfy certain quality criteria [Schatzmann et al. 1997, Schatzmann and Leitl 2011]. This paper presents a case study in which the dispersion of CO_2 in

the Amsterdam ArenA football stadium and its removal by natural ventilation are modeled using CFD, and in which the CFD simulations are validated by comparison with full-scale experiments. The validated CFD model can be used in future studies to assess indoor pollutant concentration gradients. These gradients indicate how good the enclosure is ventilated and provides information on stagnant regions, short-circuiting, etc. The Amsterdam ArenA is a multifunctional stadium that hosts a wide variety of activities, such as football games, concerts, conferences and festivities. During these activities, the roof is closed, and natural ventilation can only occur through the relatively small ventilation openings in the stadium facade. The CFD simulations in this paper are performed in a fully coupled way, i.e. outdoor and indoor air flow are modeled simultaneously in the same computational domain. This study is an extension of the earlier study with the same computational model [van Hooff and Blocken 2010]. It presents a further validation of this model for the specific complex situation after the concerts, when different physical processes such as heat and mass (water vapor and CO_2) transfer interact and where this interaction determines the natural ventilation rate.

2 DESCRIPTION OF STADIUM AND SURROUNDINGS

The ArenA stadium is surrounded by several medium and high-rise buildings, with heights varying from 12 m to a maximum of 95 m for the "ABN-AMRO" office building, which is located on the south-west side of the ArenA. The aerodynamic roughness length y_0 of the surroundings, which is needed for the CFD simulations, is determined from the updated Davenport roughness classification [Wieringa 1992]. The area on the north side of the ArenA can be classified as "closed terrain" due to the urban character that is present in a radius of 10 km upwind. The estimated y_0 for this area is 1.0 m. The area on the south side can be characterized with y_0 = 0.5 m. The Amsterdam ArenA is a so-called oval stadium (Fig. 1a). The roof is dome shaped, semi-transparent and can be closed by moving two large panels with a projected horizontal area of 110 x 40 m^2 (L x W). The stand consists of two separate tiers and runs along the entire perimeter. Figures 1a-c show a detailed plan view and the two cross-sections αα' and ββ'. The exterior stadium dimensions are 226 x 190 x 72 m^3 (L x W x H). The stadium has a capacity of 51,628 seated spectators and an interior volume of about 1.2 x 10^6 m^3.

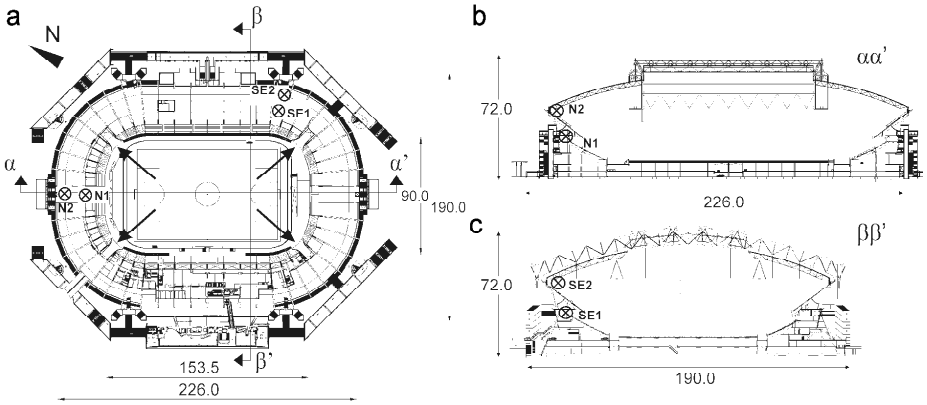

Figure 1. (a) Horizontal cross-section of stadium. The arrows indicate the four large openings (gates) in the corners of the stadium. (b) Cross-section αα'. (c) Cross-section ββ'. The four measurement positions (⊗) for air temperature, CO_2 and water vapor concentration inside the stadium are indicated. Dimensions in m.

In absence of HVAC (Heating, Ventilation and Air-Conditioning) systems, natural ventilation is the only means to ensure indoor air quality. Natural ventilation can occur through the openings that are present in the envelope of the stadium. The ArenA has several of such openings. The roof is the largest potential opening. During concerts and other festivities however, which are usually held in the summer period, the roof is closed most of the time to provide shelter to the spectators and

the technical equipment. When the roof is completely open, it is the largest opening (4,400 m^2) in the stadium envelope. When it is closed, natural ventilation of the stadium can only occur through a few smaller openings. The four gates in the corners of the stadium (Fig. 1a) together form the second largest (potential) opening (4 x 41.5 m^2). They are generally completely open. Additionally, two relatively narrow openings are present in the upper part of the stadium (Fig. 2). The first one is situated between the stand and the steel roof construction, and runs along the entire perimeter of the roof (Fig. 2a). It has a total surface area of 130 m^2. The other one is situated between the fixed and movable part of the roof (Fig. 2b). This opening is only present along the two longest edges of the stadium and has a total surface area of about 85 m^2. Of these openings, only the roof and gates can be opened/closed. In the basic configuration analyzed in this study, the roof is closed, and all other openings are open. More information on the geometry of the stadium and its surroundings can be found in van Hooff and Blocken [2010].

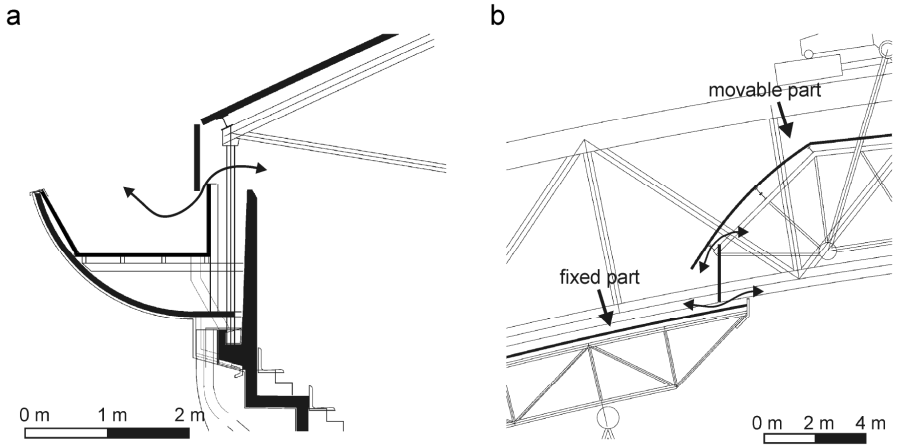

Figure 2. (a) Ventilation opening between the stand and the roof construction. (b) Ventilation opening between the fixed and the movable part of the roof.

3 FULL-SCALE MEASUREMENTS

3.1 Wind velocity

For CFD validation purposes, the 3D wind velocity in and around the stadium was measured in the period September-November 2007, on days with strong winds (reference wind speed above 8 m/s). Measurements were made with ultrasonic anemometers, positioned on mobile posts, at a height of 2 m above the floor. The measurement positions included the four openings (gates) in the corners of the stadium. Reference wind speed ($U_{ref;\,meas}$) was measured on top of a 10 m mast on the roof of the 95 m high ABN-AMRO office building, which is the highest building in the proximity of the stadium. The data were sampled at 5 Hz, averaged into 10-minute values and analyzed. Only data with at least 12 different 10-minute values per wind direction sector of 10° were retained. The measurement results will be reported together with the simulation results in section 5.1.

3.2 CO_2, temperature and vapor concentration decay

To assess the natural ventilation in the stadium, CO_2 measurements were performed at four different locations (Fig. 1a-c) and converted to air change rates per hour (ACH) using the concentration decay method:

$$ACH = \frac{\ln C(\tau_0) - \ln C(\tau_1)}{\tau_1 - \tau_0} \quad (1)$$

where ACH is expressed in h^{-1}, $C(\tau_0)$ is the concentration at time 0 in ppm, $C(\tau_1)$ the concentration at τ_1 in ppm and $(\tau_1-\tau_0)$ the time between the two measurements. The CO_2 concentration at the four positions was measured during three consecutive days on which concerts took place: June 1st, 2nd and 3rd. The analysis of the measurements is focused on the period following each of the concerts (0:00 – 2:30 am), when the CO_2 concentration had reached a maximum level caused by the attendants. The indoor air temperature and vapor concentration were measured simultaneously at the same four locations (Fig. 1). Furthermore, the outdoor air temperature and vapor pressure were measured. The outdoor temperature during the CO_2 measurements on all evenings was about 19˚C and the indoor air temperature was about 26˚C at the end of the concerts and decayed to about 19˚C at 2:30 am. The water vapor concentration decayed from 15 g/kg to 10 g/kg. From 0:00 – 2:30 am, the potential mean wind speed U_{10} measured by the Dutch Meteorological Institute (KNMI) at Schiphol airport was about 3.5 m/s and the wind direction on the three days was about 40° from north. Because of the similar conditions, the measured ACH values for these three nights were averaged. Although differences are present between the four measurement positions, and also between the three consecutive evenings, the total average ACH was around 0.67 h^{-1} with a relatively small maximum deviation of about ±10% for the values at each individual position. The ACH values based on the CO_2 concentration decay curves on three consecutive evenings were within 8% of the average ACH value for each particular position.

4 CFD SIMULATIONS: COMPUTATIONAL MODEL AND PARAMETERS

4.1 Model geometry and computational domain

The computational model of the stadium reproduces its geometrical complexity with high resolution, down to details of 0.02 m. This is required to accurately model the flow through the narrow ventilation openings (Fig. 2a,b). The computational domain has dimensions L x W x H = 2,900 x 2,900 x 908.5 m^3. The maximum blockage ratio is 1.6%, which is well below the recommended maximum of 3-5% [Franke et al. 2007, Tominaga et al. 2008]. The distance from the building to the sides, to the inlet and to the top of the domain is at least five times the height of the building and the distance from the building to the outlet is fifteen times the height [Franke et al. 2007, Tominaga et al. 2008].

4.2 Computational grid

The computational grid consists of 5.6 million prismatic and hexahedral cells. The grid is a hybrid grid; it is partially structured and partially unstructured. Special attention was paid to the precise modeling and high grid resolution of the ventilation openings of the stadium. A high grid resolution is used in the proximity of these openings in order to accurately model the flow. A grid-sensitivity analysis was performed with grids containing 3.0 million, 5.6 million and 9.2 million cells, indicating that the 5.6 million grid provides fairly grid-independent results. The specific procedure that was used to construct this body-fitted grid and the grid-sensitivity analysis are reported in van Hooff and Blocken [2010]. Some parts of the computational grid are displayed in Figure 3a,b.

4.3 Boundary conditions

At the inlet of the domain a logarithmic mean wind speed profile representing a neutral atmospheric boundary layer is imposed with an aerodynamic roughness length y_0 of 0.5 m and 1.0 m, depending on the wind direction, and a reference wind speed U_{10} at 10 m height of 3.5 m/s. The corresponding turbulent kinetic energy and the turbulence dissipation rate profiles are also imposed [van Hooff and Blocken 2010]. Note that no time-dependent velocity fluctuations are imposed at the inlet. The roughness of the bottom of the domain is taken into account by imposing appropriate values for the sand-grain roughness k_S and the roughness constant C_S in the standard wall functions [Launder and Spalding 1974, Cebeci and

Bradshaw 1977]. For Fluent 6, these parameters are calculated from the aerodynamic roughness length using $k_S = (9.793y_0)/C_S$ [Blocken et al. 2007]. The value for C_S is set equal to 7 with a user defined function (UDF) in the Fluent 6.3.26 code and the sand-grain roughness k_S is taken equal to 0.7 m. More information on this matter is provided in [Blocken et al. 2007]. For the ground surface in the direct vicinity of the explicitly modeled buildings and the stadium, $y_0 = 0.03$ m, which is imposed by setting $k_S = 0.59$ m and $C_S = 0.5$. Zero static pressure is set at the outlet of the domain and the top is modeled as a slip wall (zero normal velocity and zero normal gradients of all variables). The boundary conditions for the CO_2 dispersion simulation will be presented in section 5.2.

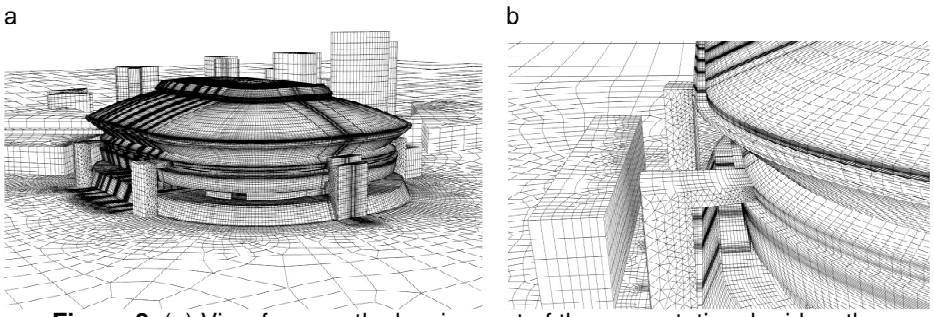

Figure 3. (a) View from north showing part of the computational grid on the surfaces of the stadium and its surroundings. (b) Bird-eye view of the grid on the southeast side of the stadium.

4.4 Other computational parameters

The 3D steady and unsteady RANS equations are solved in combination with the realizable k-ε turbulence model [Shih et al. 1995] using the commercial CFD code Fluent 6.3.26 [2006]. The realizable k-ε turbulence model is chosen because of its general good performance for wind flow around and inside buildings [Linden 1999, Franke et al. 2004]. Pressure-velocity coupling is taken care of by the SIMPLE algorithm, pressure interpolation is standard and second-order discretization schemes are used for both the convection terms and the viscous terms of the governing equations. The Boussinesq approximation is used for thermal modeling.

5 CFD SIMULATIONS: RESULTS

5.1 Wind velocity

For validation purposes a set of steady RANS simulations is performed without thermal effects and without incorporation of CO_2 and vapor concentration, because the conditions during the wind velocity measurements (i.e. strong wind conditions) are reproduced. The simulated and measured mean wind speed ratio and mean wind direction in the four gates (A, B, C, D) are compared. The mean wind speed ratio is defined as the magnitude of 3D mean velocity vector at the measurement position divided by the reference mean wind speed U_{ref} measured on top of the ABN-AMRO office building. This ratio is also calculated with CFD and both ratios are compared in Figure 4. For brevity, results are only shown for wind direction φ = 228˚. The computed mean wind speed ratio in general lies within 25% of the measured mean wind speed ratio. Given the complexity of the stadium and its surroundings, this can be regarded as a fair to good agreement. The same holds for the computed local mean wind directions in the gates (Fig. 4b), which generally are within 10° of the measured wind directions, except for gate D. In this gate, the CFD simulation predicts a flow parallel to the opening, whereas the measurements showed flow directed into the stadium (90° deviation). This can probably be attributed to the presence of slender columns close to this measurement position, which were not included in the CFD model. Overall, a fair agreement between simulations and measurements is obtained.

5.2 CO_2 dispersion and removal

These simulations are intended to reproduce the conditions at the end of the concerts (0:00 – 2:30 am), as described in section 3.2. Two consecutive simulations are performed. First, steady RANS is used to calculate the steady-state wind-flow pattern in and around the stadium, to be used as initial condition for the transient simulations. Next, unsteady RANS CFD simulations of wind flow and the decay of air temperature, CO_2 and water vapor concentration are performed. The initial values for temperature, vapor and CO_2 concentration outside and inside the stadium are set to the measured values at the beginning of the CO_2 measurements. The indoor air temperature at the beginning of the CO_2 decay simulation is set to 26ºC, the outdoor temperature is set equal to the measured value of 19°C. The surface temperatures are assumed to be equal to the indoor temperature, which is a simplification of the real surface temperatures that will have been slightly higher. The CO_2 concentration inside the stadium is set to the measured maximum value of 2000 ppm (uniformly distributed) and the concentration outside the stadium is set to 400 ppm. The indoor water vapor pressure is set on 15 g/kg whereas the ambient water vapor pressure is set on 10 g/kg. To incorporate the effect of changing air temperatures and water vapor concentrations on the flow field the momentum equations are solved simultaneously with the species transport and energy equations. The time step is 30 seconds. Note that the overall decay of air temperature, water vapor and CO_2 concentration are of primary interest in this study, and not the short-term velocity fluctuations, which would have required smaller time steps.

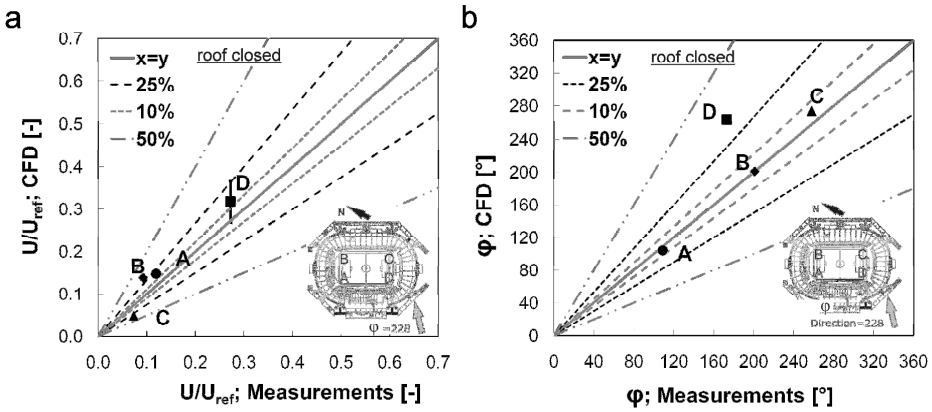

Figure 4. Comparison between numerical and experimental results in the four gates A, B, C and D, for closed roof and reference wind direction φ of 228º. (a) Dimensionless mean wind speed ratio U/U_{ref}; (b) local mean wind direction φ.

5.3 Results

Figure 5 shows the measured CO_2 concentration decay at position N2 as well as the simulated CO_2 concentration decay for five different positions: the four measurement positions and the middle of the stadium interior. The CO_2 concentration decay curve at N2 obtained with the CFD simulations shows a fair agreement with the measured decay curve. The average deviation in CO_2 concentration amounts 8.2%. Furthermore, the ACH based on the CFD simulations is 0.64 h^{-1}, which corresponds well to the measured averaged ACH value of 0.67 h^{-1} (difference < 5%). Positions N1, SE1 and "Middle" show a larger deviation, but overall these curves show a fair to good agreement with the measurements as well. One possible explanation for the larger deviations at these three positions is that they are all located at a relatively large distance from the ventilation openings, while positions N2 and SE2 are located in the close vicinity of the ventilation openings near the gutter. In this area the wind will dominate the flow, whereas inside the stadium buoyancy will be more important. Since the surface temperatures inside

the stadium are slightly lower than the ones in reality, small deviations can be present with respect to the buoyancy-driven flow inside the stadium.

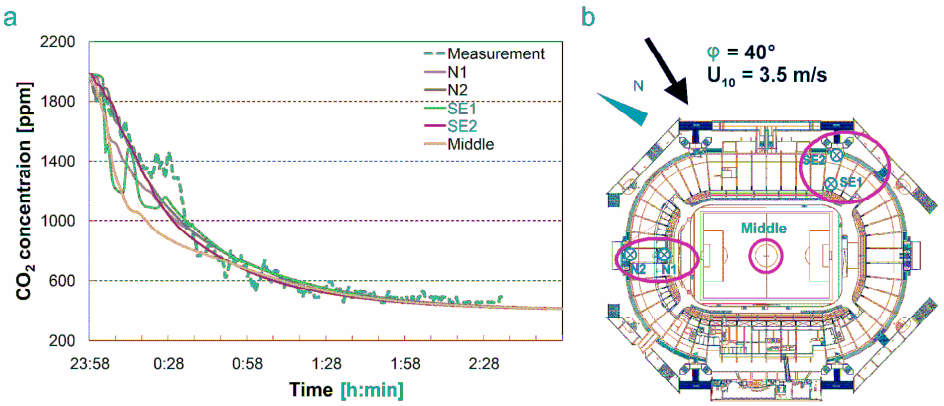

Figure 5. (a) Measured CO_2 decay (dotted line) for position N2 and simulated CO_2 decay (continuous lines) using URANS for five different positions inside the stadium. (b) Positions for the measurements and/or simulations.

6 SUMMARY AND CONCLUSIONS

High-resolution CFD simulations and full-scale measurements have been performed to assess the dispersion of air pollutants from the large semi-enclosed Amsterdam ArenA football stadium. The following conclusions are made:

- Wind velocity measurements have been used as a first validation step for the CFD model of the stadium and its surroundings and a fair agreement between simulations and measurements has been found.
- A grid-sensitivity analysis for the wind velocity through the gates as main ventilation openings has been performed, which has resulted in a grid with 5.6 million cells.
- CFD simulations of CO_2 concentration decay have been made and they have been compared with measurement results, and a fair to good agreement has been obtained.
- This study is only a first step. Further research will consist of additional investigations into the sensitivity of CFD indoor dispersion and natural ventilation results to the wide range of computational parameters.
- The validated CFD model will be used in future research for a detailed evaluation of indoor concentration gradients and the interaction between wind-induced and buoyancy-induced natural ventilation.

ACKNOWLEDGEMENTS

Twan van Hooff is currently a PhD student funded by both Eindhoven University of Technology in the Netherlands and Fonds Wetenschappelijk Onderzoek (FWO) - Flanders, Belgium (FWO project number: G.0435.08). The FWO Flanders supports and stimulates fundamental research in Flanders. Its contribution is gratefully acknowledged.

REFERENCES

Blocken, B., T. Stathopoulos, and J. Carmeliet, CFD simulation of the atmospheric boundary layer: wall function problems, *Atmospheric Environment*, 41(2), 238-252, 2007.

Blocken, B., W.D. Janssen, and T. van Hooff, CFD simulation for pedestrian wind comfort and wind safety in urban areas: General decision framework and case

study for the Eindhoven University campus, *Environmental Modelling & Software*, 30, 15-34, 2012.

Blocken, B., and C. Gualtieri, 2012. Ten iterative steps for model development and evaluation applied to Computational Fluid Dynamics for Environmental Fluid Mechanics, *Environmental Modelling & Software,* 33, 1-22, 2012.

Casey, M., and T. Wintergerste, *Best Practice Guidelines*, ERCOFTAC Special Interest Group on Quality and Trust in Industrial CFD, ERCOFTAC, Brussels, 2000.

Cebeci, T., and P. Bradshaw, *Momentum transfer in boundary layers*, Hemisphere Publishing Corporation, New York, 1977.

Chen, Q., Ventilation performance prediction for buildings: A method overview and recent applications, *Building and Environment* 44(4), 848-858, 2009.

Fluent Inc., *Fluent 6.3 User's Guide*. Fluent Inc., Lebanon, 2006.

Franke, J., A. Hellsten, H. Schlünzen, and B. Carissimo, *Best practice guideline for the CFD simulation of flows in the urban environment*, COST 732: Quality Assurance and Improvement of Microscale Meteorological Models, 2007.

Franke, J., C. Hirsch, A.G. Jensen, H.W. Krüs, M. Schatzmann, P.S. Westbury, S.D. Miles, J.A. Wisse, and N.G. Wright, Recommendations on the use of CFD in wind engineering. *Proceedings of the International Conference on Urban Wind Engineering and Building Aerodynamics*, COST Action C14, Impact of Wind and Storm on City Life Built Environment. Von Karman Institute, Sint-Genesius-Rode, Belgium, 5–7 May 2004.

Heiselberg, P., Y. Li, A. Andersen, M. Bjerre, and Z. Chen, Experimental and CFD evidence of multiple solutions in a naturally ventilated building, *Indoor Air*, 14(1), 43-54, 2004.

Hunt, G.R., and P.F. Linden, The fluid mechanics of natural ventilation - displacement ventilation by buoyancy-driven flows assisted by wind, *Building and Environment*, 34(6), 707-720, 1999.

Jakeman, A.J., R.A. Letcher, and J.P. Norton, Ten iterative steps in development and evaluation of environmental models. *Environmental Modelling & Software,* 21(5), 602-614, 2006.

Launder, B.E., and D.B. Spalding, The numerical computation of turbulent flows. *Computer Methods in Applied Mechanics and Engineering*, 3, 269-289, 1974.

Li, Y.G., and A. Delsante, Natural ventilation induced by combined wind and thermal forces, *Building and Environment*, 36(1), 59-71, 2001.

Linden, P.F., The fluid mechanics of natural ventilation, *Annual Reviews of Fluid Mechanics*, 31: 201-238, 1999.

Ramponi, R., and B. Blocken, CFD simulation of cross-ventilation for a generic isolated building: impact of computational parameters, *Building and Environment*, 53, 34-48, 2012.

Schatzmann, M., S. Rafailidis, and M. Pavageau, Some remarks on the validation of small-scale dispersion models with field and laboratory data, *Journal of Wind Engineering and Industrial Aerodynamics* 67&68, 885-893, 1997.

Schatzmann, M., and B. Leitl, Issues with validation of urban flow and dispersion CFD models. *Journal of Wind Engineering and Industrial Aerodynamics*, 99(4), 169-186, 2011.

Shih, T.H., J. Zhu, and J.L. Lumley, A new Reynolds stress algebraic equation model, *Computer Methods in Applied Mechanics and Engineering*, 125, 287–302, 1995.

Tominaga, Y., A. Mochida, R. Yoshie, H. Kataoka, T. Nozu, M. Yoshikawa, and T. Shirasawa, AIJ guidelines for practical applications of CFD to pedestrian wind environment around buildings, *Journal of Wind Engineering and Industrial Aerodynamics* 96(10-11), 1749-1761, 2008.

van Hooff, T. and B. Blocken, B., Coupled urban wind flow and indoor natural ventilation modelling on a high-resolution grid: A case study for the Amsterdam ArenA stadium, *Environmental Modelling & Software*, 25(1), 51-65, 2010.

Wieringa, J., Updating the Davenport roughness classification, *Journal of Wind Engineering and Industrial Aerodynamics*, 41-44, 357-368, 1992.